

# NUMERICAL STUDY AND EXPERIMENTAL VALIDATION OF THE WATER FILMS AND THE DETACHMENT OF DROPS ON DRIFT ELIMINATORS

J. López<sup>1</sup>, A. S. Kaiser<sup>1\*</sup>, B. Zamora<sup>1</sup>, M. Lucas<sup>2</sup>, J. Ruiz<sup>2</sup> A.Viedma<sup>1</sup>

<sup>1</sup>Dpto. de Ingeniería Térmica y de Fluidos. Universidad Politécnica de Cartagena.

<sup>2</sup>Dpto. de Ingeniería Mecánica y Energía. Universidad Miguel Hernández.

\*Author for correspondence

Dr. Antonio Sanchez Kaiser

c/ Dr. Fleming s/n, 30202 Cartagena (Murcia), Spain

E-mails: [javilo08@hotmail.com](mailto:javilo08@hotmail.com),

[antonio.kaiser@upct.es](mailto:antonio.kaiser@upct.es),

[blas.zamora@upct.es](mailto:blas.zamora@upct.es),

[mlucas@umh.es](mailto:mlucas@umh.es),

[j.ruiz@goumh.umh.es](mailto:j.ruiz@goumh.umh.es),

[antonio.viedma@upct.es](mailto:antonio.viedma@upct.es)

Keywords: Multiphase flow, VOF model, Cooling tower

## ABSTRACT

This paper is focused on the study of a type of drift eliminator installed in a mechanical draft cooling tower. Drift eliminators are installed in cooling towers in order to avoid water droplets to be emitted to the ambient. These droplets are formed by the crossflow between airflow and water pulverization inside the tower.

The study is centered on the analysis of three aspects: the water film formed on the plates of the drift eliminator, the size of water droplets detached from this film and the flow conditions for the detachment of these droplets. These aspects are studied with a multiphase numerical approach, validated by experimental tests. Good agreement is obtained between numerical and experimental results. The study shows that the behavior of water droplets is very influenced by air velocity inside the cooling tower. Moreover, limits for air velocity are set for the drift eliminator not to act as a droplet generator itself.

## INTRODUCTION

Mechanical draft cooling towers are components for heat dissipation in air conditioning systems. Its operating principle is based on the adiabatic evaporation of a small part of the circulating water, cooling the rest. The water enters the cooling tower by spray, or by free fall, into a crossflow airstream. The adiabatic evaporation of a small part of the water induced by the contact with the air results in the cooling of the rest of the water collected in a lower tank (Lucas et al., 2013).

The efficiency of cooling towers is higher than any other alternative cooling system. However, the use of these devices is limited because they can release into the environment drops of water (a phenomenon called drift), which may contain harmful chemicals or microorganisms. Drift eliminators are installed inside the tower in order to reduce the release of water drops into the environment through the impact of these drops on drift eliminator's plates (Zamora and Kaiser, 2012).

Drift eliminators are made up of several plates placed inside the cooling tower forming angles, so that water droplets can collide with them and not follow the airstream to outside. The changes of direction caused by the plates generate pressure losses that can lead to the reduction of the heat exchange within the tower, or the increase of the air vent's power needed. In any case, they result in a reduction of the global cooling system efficiency. The rate of drift loss is a function of tower configuration, eliminator design, airflow rate through the tower and water loading.

Several types of drift eliminators have been studied to evaluate their efficiency. James et al. (2005) studied numerically the behavior of two plates forming a canal with six bends. In this case, they studied a mist eliminator: a device used in the process industry to separate liquid from a gas stream, and not to transfer heat, but mist and drift eliminators operate on the same basis: liquid droplets impact on the plates, accumulate and form thin films. Zamora and Kaiser (2012) evaluated the efficiency of four types of wave-plate drift eliminators with different plate forms. They also calculated numerically the droplet collection efficiency for a range of airstream velocities and droplet diameters, proposing a global correlation for this collection efficiency. Lan et al. (2008) studied a water film drifted by a crossflow airstream. Moreover, Anisimov and Pandelidis (2014) studied advanced configurations of cooling towers based on indirect evaporative cooling, in which water is also drifted by a crossflow over plates.

In this way, drift eliminators designed for use in cooling towers are optimized to work effectively within the general air velocity ranges of cooling towers, 2.0-3.6m/s, and every eliminator has its own efficiency profile based on its unique design. Based on the inertial impaction theory of operation, at low velocities both the air and the drift droplets are able to pass through the eliminator due to the low inertial values of each. As the air velocity increases, the changes in direction have more impact on the drift droplets and they begin to collect on the eliminator surfaces. At the upper ranges of air velocities the air is able to re-entrain the accumulated drift water and strip it out of the eliminator, a phenomenon known as “breakthrough” (Miller, 2012).

The main objective of this work is to describe the interaction between the water film and the air flow on the plates of the drift eliminator and to determine the operating conditions for the drift eliminator to act itself as a droplet generator. This means to determine the critical values for the air flow to make water droplets, originated from the eliminator plates, to be drifted by the airstream to outside.

## **EXPERIMENTAL APPARATUS AND PROCEDURE**

### **Installation objectives and operation**

An experimental prototype of a mechanical draft cooling tower has been set up to study the interaction of air and water in a drift eliminator. This prototype consists on a prismatic structure closed by 4 lateral faces, as seen on figure 1.

The air supply system consists of one centrifugal vent (0.55 kW) and a regulator. The test section, at the central part of the tower, is removable to allow easier changes (figure 2).

The water supply system (figure3) is designed to maintain a constant value for water mass flow at the inlet placed on one of the plates of the drift eliminator. This system consists of a centrifugal pump taking water from the lower tank and pumping it to the test section. The water goes through a flowmeter before it is introduced through a slot on the plate. Once the water is on the plate, it forms a film that, in absence of a strong enough air flow, runs down falling to the porous filling and farther down to the lower tank, finally returning to the circuit.

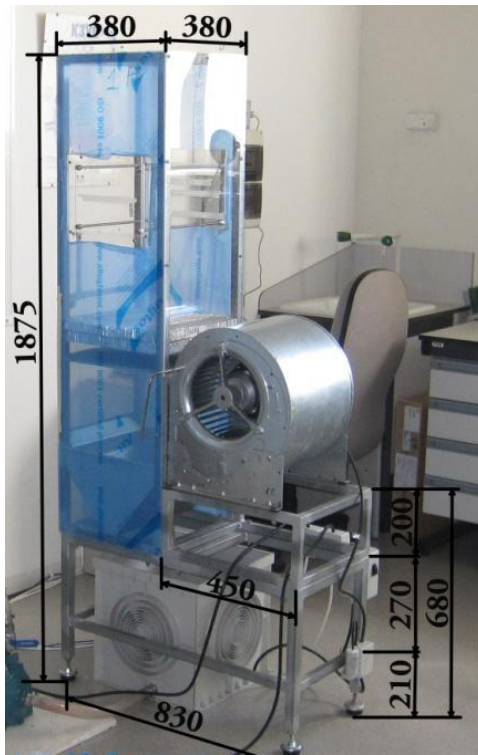


**Figure 1. Image of the studied cooling tower prototype. Units in mm.**



**Figure 2. Image of the test section including the plates of the drift eliminator.**

Water is usually sprayed below the drift eliminator and above the porous filling, however, our study is focused on the droplets generated in the drift eliminator, so the water film will be considered to be formed directly over the plate. This water film is originated in actual cooling towers when droplets from the spray gather on the plate. Then the water film is swept away by the airstream, as explained by Arienti et al., (2010) and goes up or down due to the airstream force or

gravity, respectively. Once the film gets to the edge of the plate, the detachment of droplets occurs. This is the effect that the present paper wants to assess

### Data acquisition system and uncertainty calculation

The flow variables needed to assess the operating conditions inside the cooling tower are: air velocity field, water mass flow, water film thickness and droplets size. A hot wire anemometer (model TSI 8465) is used to measure air velocity in the test section between the drift eliminator plates. A Pitot tube (model SR 305) and a differential pressure transducer (model DPT100-R2AZ-D-Span) are preferred to measure the air velocity when the water is circulating. Additionally, a flowmeter is used to measure the water flow entering the tower. All these measures are registered through a data acquisition system with a resolution of 16 bits and a maximum of 8 analogical inputs.

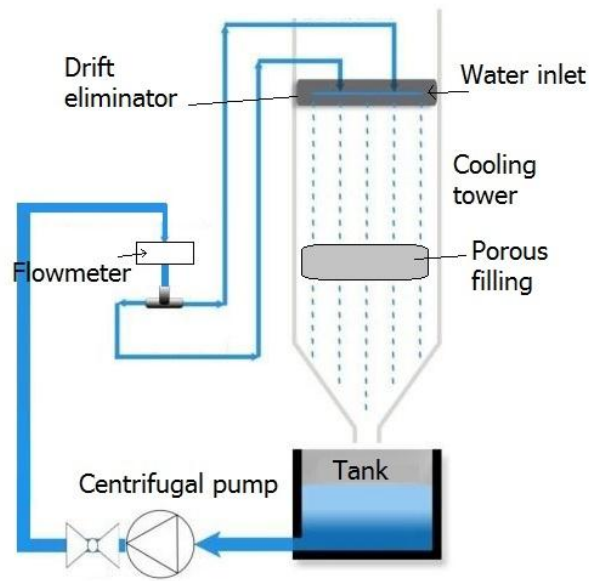


**Figure 3. Operating scheme of the cooling tower.**

The images and videos needed to measure the size of droplets and the thickness of the film were taken by a high velocity camera with a maximum velocity of 1200 fps at a resolution of 320 x 120 px. The camera used in this study is a Nikon 1 J1 model.

To calculate the uncertainty of the measurement process, the advices of the reference guide (ISO, 1995) have been followed. Total uncertainty is 0.0658 m/s for Pitot tube; 0.095, 0.138 or

0.196 m/s (depending on the selected range) for hot wire anemometer and 0.003, 0.019, or 0.036 l/min (depending on the range) for the flowmeter.

### **Experimental tests plan**

Initially, tests are carried out without water in order to measure the air velocity field in the test section. Measures are taken with the hot wire anemometer at three different heights inside the channel formed by the two plates ( $h_1$ ,  $h_2$  and  $h_3$ ) and at five different points (figure 4.b) distanced 10 mm covering the whole gap between the plates (60 mm).

Two different types of tests are carried out. First, the behavior of the crossflow and the water films are studied for four air velocities values:  $V_1$ ,  $V_2$ ,  $V_3$  and  $V_4$  (2, 4, 6 and 8 m/s respectively at the air inlet section); and also for four values of the water flow:  $Q_1$ ,  $Q_2$ ,  $Q_3$  and  $Q_4$  (0.14, 0.28, 0.67 and 2.91 l/min respectively). Some images are taken experimentally, and numerically simulated, to obtain the thickness of the water film in each case.

After that, for each value of the water flow, two limit air velocities are obtained. The first one is the limit air velocity for the droplets to get the lower edge of the plate, detach from the film and go up drifted by the airstream ( $VL_1$ ). The second one is the limit air velocity for the droplets to get the upper edge, detach from the film and go up ( $VL_2$ ).

## **NUMERICAL MODELING**

### **Computational domain**

Two types of numerical model have been implemented. First, a two-dimensional model was used to simulate the air stream and to obtain pressure and velocity fields. Although it is possible to obtain with the 2D simulations the shear stresses between air and water, and the velocity limits at which droplets begin to separate from the water film, to determine the formation of droplets it was necessary to develop a 3D model, taking the 2D simulation as a starting point. This 3D model let us to analyze the droplet detaching processes that take place in the drift eliminator.

The 2D cooling tower model was carried out with the ANSYS Design Modeler software. The model is one middle plane of the 3D tower as seen on figure 4. The domain is a rectangle of 880 x 330 mm, and the water film thickness is lower than 1 mm in many cases.

The mesh is a structured one, with elements large enough to simulate the airstream properly and get a good solution of pressure and air velocity fields, elements are 2 mm squares in the test section and 4 mm in the rest of the tower regions. But the ANSYS Fluent meshing adaption option is used to refine the mesh in zones where water appears in a volume fraction over 0.3. Figure 5a shows the mesh before including water.

The porous zone, with a height of 100 mm, is placed just above the air entrance. It is used to obtain a more uniform velocity field in the channel. In the 2D model, it is defined as a region with a porosity value of 0.8, obtained throughout the comparison between experimental and numerical results for air velocity at the entrance of the test section.

The three-dimensional model of the cooling tower is shown in figure 6. Elements in this model are 2 cm cubes filling the whole region. It consists of two different sub-models. One represents the upper edge of the plate and the nearby region and the other one the lower edge of the plate. These are the two more critical regions regarding on the detachment of droplets. Both parts are formed by a 5 cm cube enclosing partially of the plate and the edge of it.

### **Boundary conditions**

Regarding on boundary conditions, the pressure outlet condition is set on the upper base of the cooling tower with a zero value for gauge pressure. For air entrance, velocity inlet condition is used, with velocity values chosen in order to adjust airstream velocities in the channel zone to the experimental results. Finally, a velocity inlet condition is also used for water injection. The water injection surface in the installation is a 2x275 mm rectangle, so the velocity value is obtained dividing the experimental value of water flow by the area of the surface.

In 3D cases, the boundary conditions are set after the correspondent 2D case is solved. Contours of air velocity and pressure are taken from the 2D model and used in the 3D model as boundary conditions. A pressure outlet condition is set in the upper face of the model and in the rear face; velocity inlet in the air entrance and also in the water entrance; a symmetry condition is used for the rest of faces. In figure 7, the boundary conditions in 3D model are shown.

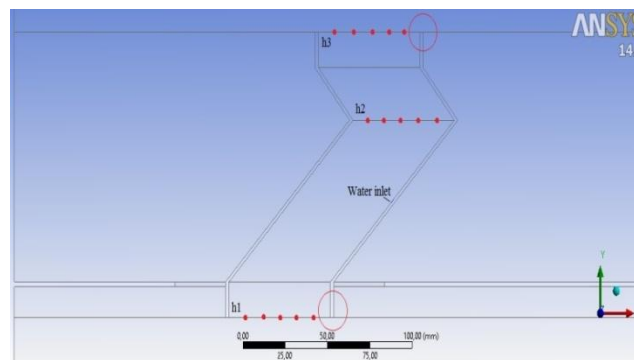
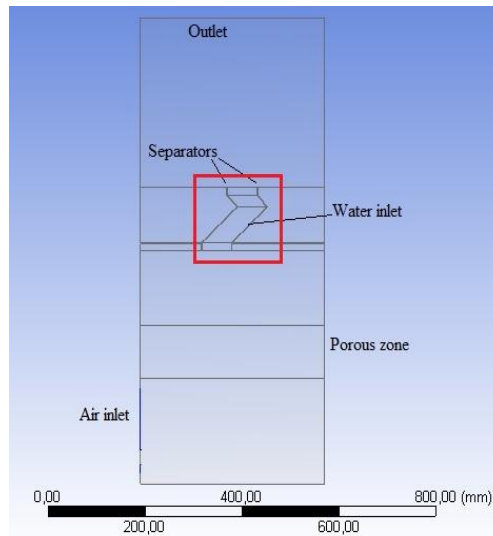


**Figure 4. (a) Schematic representation of the cooling tower. (b) Schematic representation of the channel zone: points indicate the points where experimental measures were taken at h1, h2 and h3; and circles mark the edges where detachment of droplets happens.**

### **Numerical approach**

The standard k- $\epsilon$  turbulence model is employed to simulate the air flow. For the multi-phase flow, the volume-of-fluid model was used. The VOF model can reproduce two or more immiscible fluids by solving a single set of momentum equations and tracking the volume fraction of each of the fluids throughout the domain. With regard to numerical convergence, for each time step, the criterion is a value for the continuity residual of  $5 \cdot 10^{-6}$ .



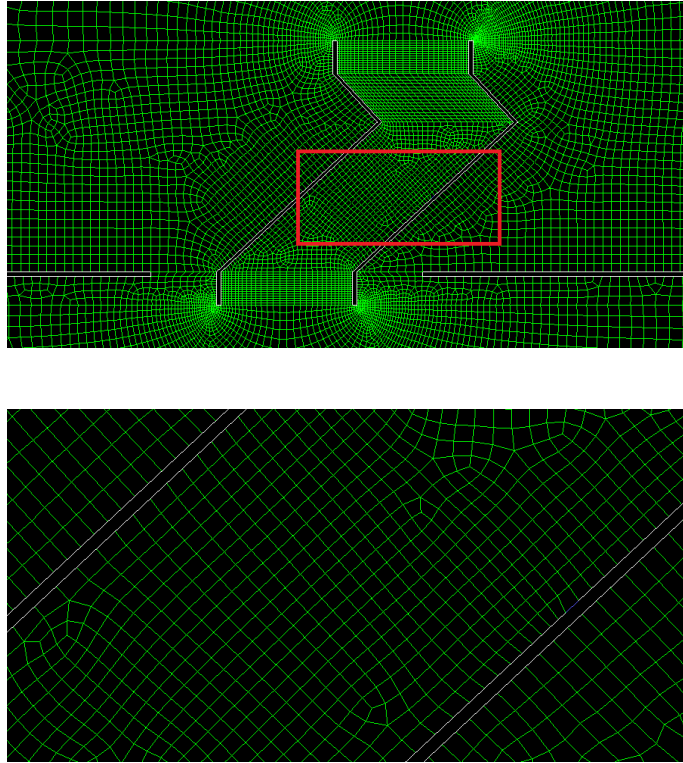


**Figure 5. (a) Mesh used for the channel zone. (b) Detail of element size in the channel zone, note that the thickness of plates is 2 mm.**

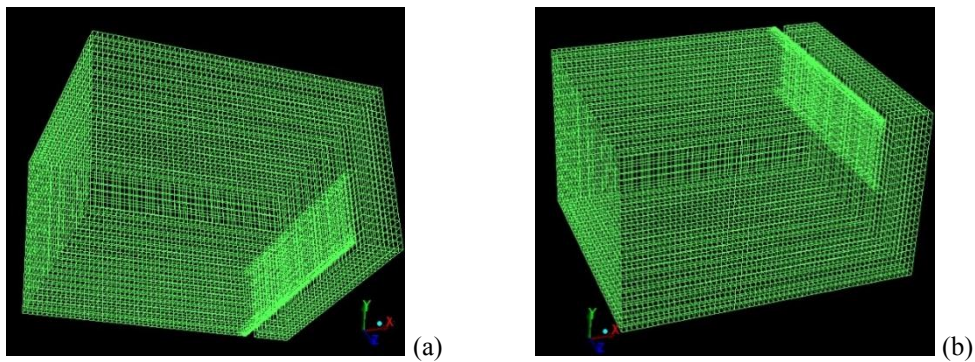


**Figure 6. 3D Mesh of the upper edge (a) and the lower edge (b).**

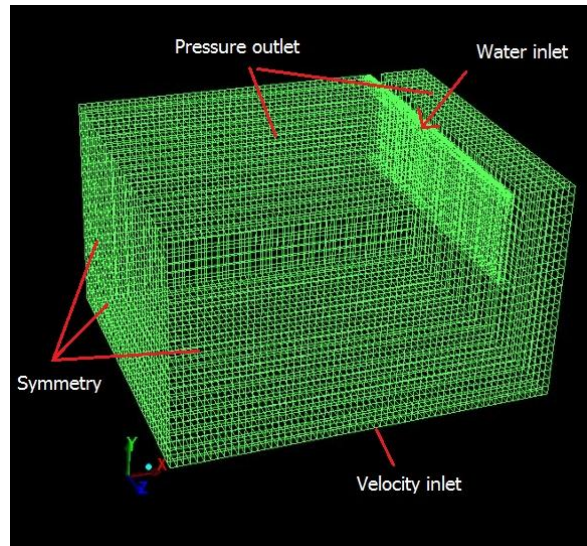


**Figure 7. 3D boundary conditions.**

The Compressive Interface Capturing Scheme for Arbitrary Meshes (*CICSAM*) solution method is used in the simulations. It is a high resolution differencing scheme, particularly suitable for flows with high ratios of viscosities between the phases (Fluent 14 guides, 2013). Surface tension effects between air and water are also considered in the simulations. Wall adhesion is enabled and a study for surface tension has been done: three different values for surface tension have been tested. Taking into account the previous studies from James et al. (2005) in which a value of 0.078 N/m was set, numerical cases were simulated with values 0.06, 0.072 and 0.08 N/m. Next figures 8, 9 and 10 show water film thickness for these cases. The results were compared with experiments and a surface tension value of 0.06 N/m was chosen to obtain the best possible fit between numerical and experimental results.

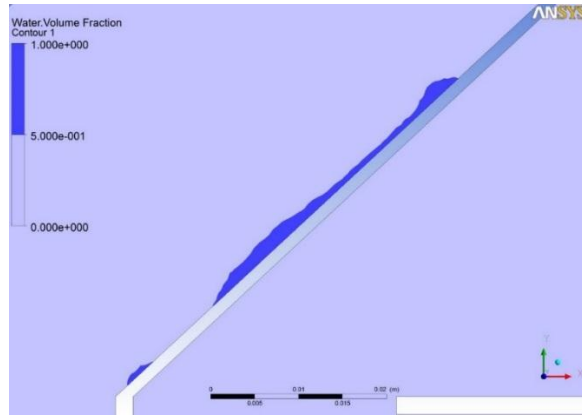


**Figure 8. Water film for 0.06 N/m of surface tension.**

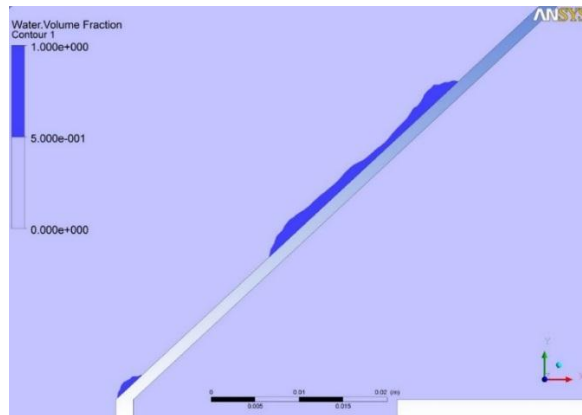


**Figure 9. Water film for 0.08 N/m of surface tension.**

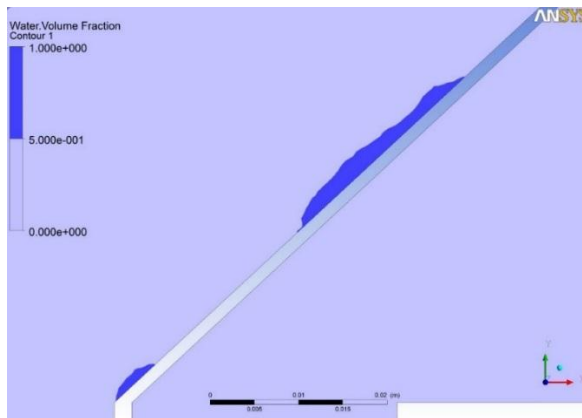


**Figure 10. Water film for 0.072 N/m of surface tension.**

Moreover, the contact angle between water, air and the plate was set in  $45^\circ$  and the roughness of the plate was also considered. Both contact angle and wall roughness were adjusted looking also for the best possible fit between numerical and experimental results.

Once the simulation with just air is converged in a steady state simulation, then a transient simulation is carried out. It is important to set the Courant number properly regarding on convergence: it relates the size of cells forming the interface with the time step size. The Courant number is set in 0.01 and the initial time step size is  $8 \cdot 10^{-6}$  seconds, both parameters were set through a number of previous testing simulations, in order to reach the proper solution in an optimal computation time. The time step size is so small due to the size of the cells in the interface zone (less than 500 microns).

## **RESULTS AND DISCUSSION**

A comparison of the experimental and numerical results for air velocity field, water film thickness and the flow conditions that cause the detachment of droplets is carried out in this study and presented in the next points.

### **Air velocity fields**

First, the validation for air flow velocities is done comparing the experimental data from the prototype and the numerical results in the same sections of the channel. Figure 11 shows an example of the numerical results for the air velocity magnitude field. In this figure, zones with high air velocities can be seen forming a preferential path, while others areas present much lower velocity levels and a higher pressure.

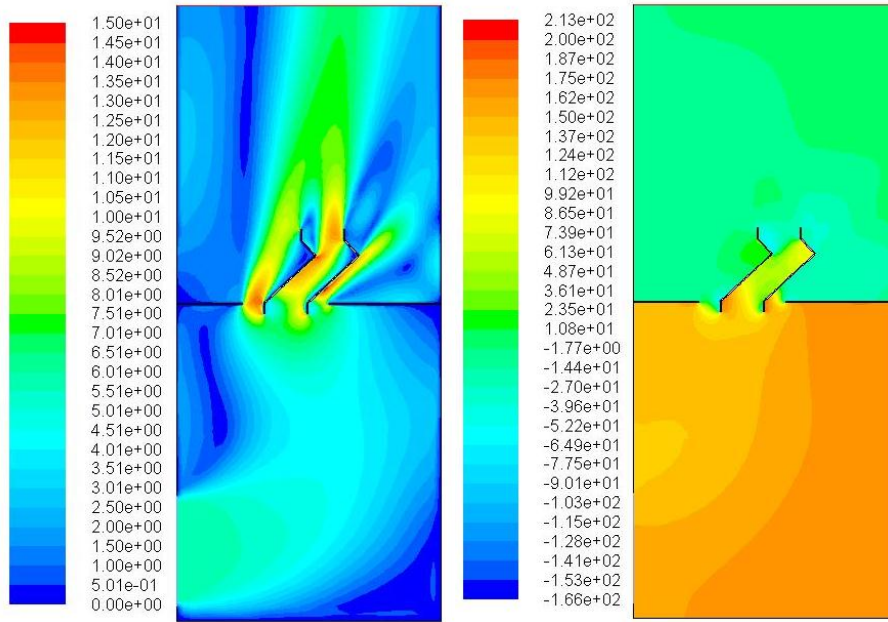


**Figure 11. Example of air velocity in m/s (left) and pressure in Pa (right) fields in the test section.**

Figures 12 to 15 show that a good agreement is achieved for the general trends between the numerical and the experimental velocity profiles. The velocity inlet boundary condition was obtained testing air velocities at the inlet and comparing the result with the experimental ones. In general, the values for numerical and experimental air velocities have a maximum difference of 20%. The lower height in the channel zone ( $h_1$ ) present more homogeneous air velocities due to the porous filling placed under the drift eliminators. The highest disagreement is shown in figures 14 and 15 for the  $h_3$  height profile. It may be caused by the three dimensional nature of the flow at this section.

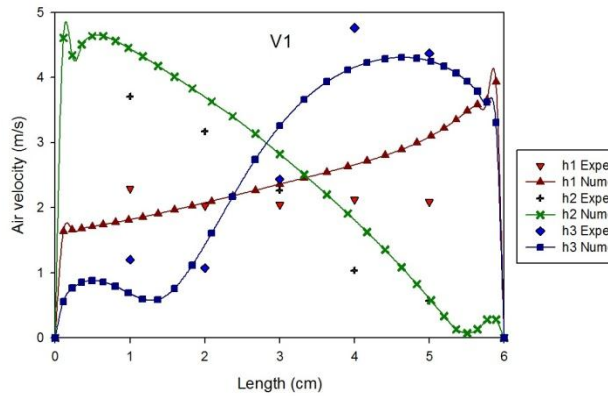


**Figure 12. Air velocities for V1 at the air entrance section.**

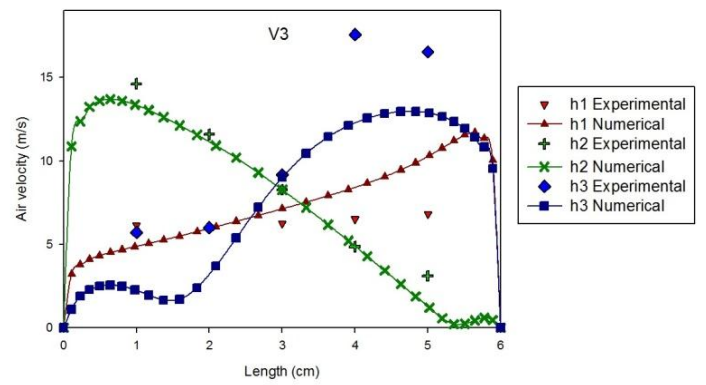


**Figure 14. Air velocities for V3 at the air entrance section.**

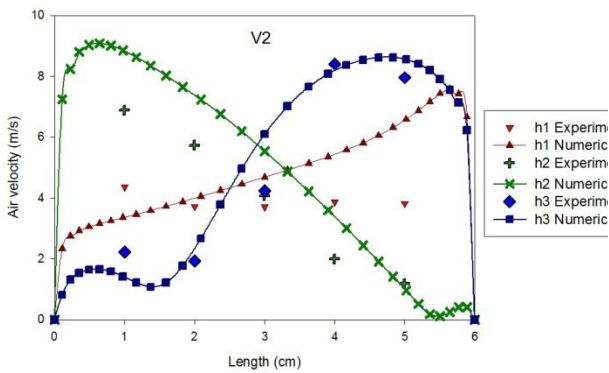


**Figure 13. Air velocities for V2 at the air entrance section.**

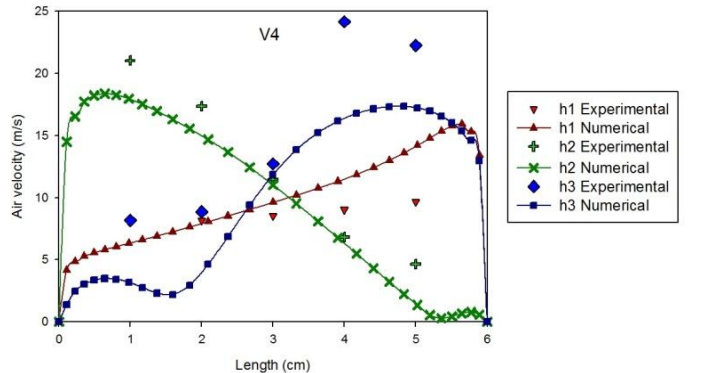


**Figure 15. Air velocities for V4 at the air entrance section.**

### Water film and detached droplets

Once the air flow is fully resolved, the liquid phase is included in the problem. In figure 16, a comparison between experimental and numerical results for the water film thickness is presented as a function of the air velocity, for two different flow rates: Q3 and Q4. It can be observed that values for water film thickness are simulated with an error lower than 5 %. The used images are taken from one side of the tower, as seen on figure 17, capturing the whole thickness of the film. This thickness is measured through the processing of the images with a software Developed for this purpose. Regarding the numerical case, the interface criterion is set in 0.5 of water volume

fraction so that the quantity of water included in the film is enough to get an accurate estimation of the interface (Lan et al., 2008).

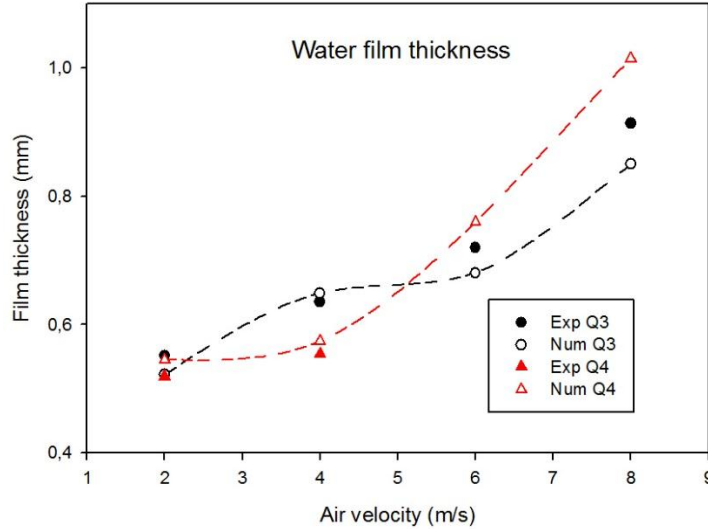


**Figure 16. Water film thickness in cases for Q3 and Q4 and the four different values for air velocity.**

The results of figure 16 show the increase of the water film thickness as the air velocity is higher. The influence of water flow rate is not so clear, as far as the thickness for different values of water flow rate do not show significant differences. These results are similar to the ones obtained by Zhou et al. (2009), in which the measurement of water film thickness is presented as a function of the Reynolds number, (related to air velocity). An example of an image taken to measure the film thickness can be seen before processing in figure 17.

More than 600 images were digitally analyzed to study the process of droplet generation from the plates of the drift eliminator. The ranges of droplet diameters for three water flow rate and four air velocities are included in table 2 and 3. Table 2 correspond to the lower edge of the plate (velocities V1 and V2), while table 3 correspond to the upper plate edge (velocities V3 and V4). These ranges may be influenced by different aspects such as the ability of the camera, the size of the domain or the maximum recording time interval chosen. In spite of obtaining ranges of droplet sizes in the order of millimeters, it is expected that lower droplet diameters can occur.

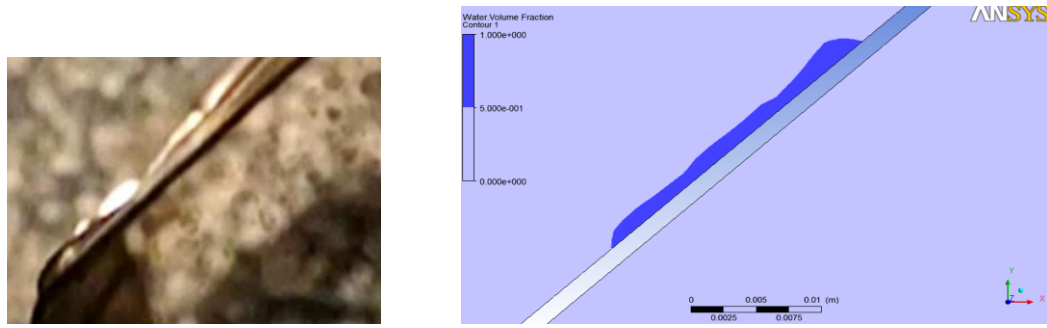


**Figure 17. Images of experimental and numerical water film over the plate.**

In the cases with higher air velocities, water film breaks into smaller droplets due to the higher shear forces of air on the water surface. Otherwise, droplets are higher when water flow increases. The water film thickness is higher when air velocity increases; the explanation for that is based on the force that airstream performs on the water film. That force slows down the water and makes its thickness increase.

It is important to highlight that 2D simulations are used to obtain water film thickness or the detachment of this film from the plate. However, regarding on droplets, it is necessary to use 3D simulation as far as a drop is always three-dimensional (figure 20).

**Table 1. Droplet diameter range in mm for droplets falling from the separator plate.  
\*Difficulties to measure a single drop.**

		Q1 (0.14 l/min)	Q2 (0.28 l/min)	Q3 (0.69 l/min)	Q4 (2.91 l/min)
V1 (2 m/s)	Min	1.23	1.71	0.84	*
	Max	6.82	7.06	7.16	*
V2 (4 m/s)	Min	0.74	1.24	1.17	0.71
	Max	8.23	8.93	9.36	9.56



**Table 2. Droplet diameter in mm for droplets leaving the separator in the upper zone.  
\*Difficulties to measure a single drop.**

		Q1 (0.14 l/min)	Q2 (0.28 l/min)	Q3 (0.69 l/min)	Q4 (2.91 l/min)
V3 (6 m/s)	Min	0.36	0.96	0.72	0.66
	Max	1.96	4.10	4.29	4.29
V4 (8 m/s)	Min	*	0.86	0.61	0.64
	Max	*	3.31	3.01	2.94



**Figure 18. Image of experimental droplets leaving the separator plate. The experimental case is the V1Q1.**

### **Velocity limits**

Results for air velocity field, water film thickness or droplet size are useful in order to validate the numerical model; however, what is more relevant is to determine the maximum air velocity that can be set in the cooling tower, so that water is not released into the environment. Tests for all the water flow rate studied have been done experimentally. There are two different critical or limit situations: when the water film reaches the upper edge (VL2) of the separator plate or when the water reaches the lower one (VL1). In both cases water drops can separate from the film and fall down, or be detached and released into the environment. An air velocity limit exists for any mass flow rate considered, as shown in table 4. When air velocity is higher than VL2 at the outlet of the channel, water drops are released into the environment. It is possible to have high velocities at the outlet of the channel (height  $h_3$ ) with moderate air velocities at the entrance (height  $h_1$ ) due to the

acceleration of the air (figures 12 to 15). When air velocity is higher than VL1 at the inlet of the channel, the water film falling down at the lower edge of the plate, break into small droplets that are incorporated into the air upward stream and are eventually released into the environment.

**Table 3. Limit air velocities for every water flow, where VL1 represents the cases when water reaches the lower edge of the plate; and VL2 when water reaches the upper edge.**

	VL1 (m/s)	VL2 (m/s)
Q1	4.55	13.71
Q2	4.36	12.98
Q3	4.34	11.30
Q4	4.34	12.50

Numerical simulations have been carried out in order to be compared with these results. Figure 19 represents the Q4 case; it means the highest value for water flow rate.

To obtain the limit velocity, several simulations are carried out with the same value for the water flow and testing different air velocities at the inlet, until the detachment of droplets happens. A final value of 8.5 m/s is set as the inlet air boundary condition. This value causes an air velocity of 12.6 m/s at the point where experimental measures are taken at height h3. In table 4, the value for VL2, for the same Q4, is 12.5 m/s (0.8 % error).

Figure 19 shows how water drops are detached from the film, leave the plate and enter the main airstream to get out of the tower.

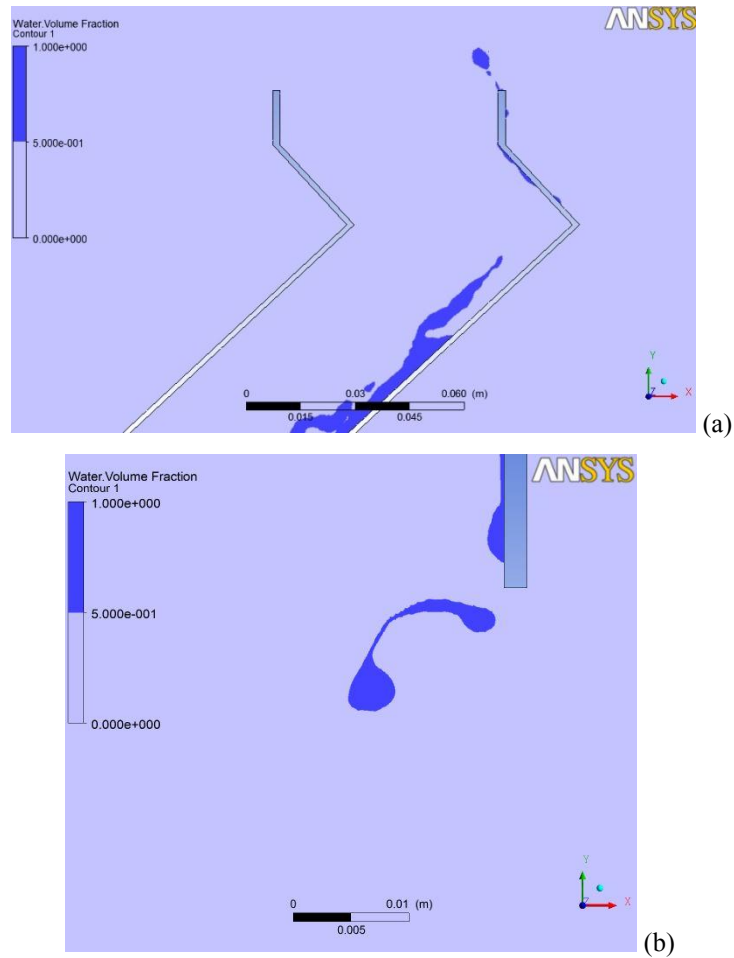


**Figure 19. (a) Water volume fraction for VL2-Q4 case.  
 (b) Water volume fraction for VL1-Q4 case.**

### **3D simulation of re-entrainment of the water film**

Once the film reaches the lower edge of the plate, the airstream drags the droplets and make them to separate from the film. These droplets can go down to the bottom of the tower or can go up and leave the tower, which is the problem to prevent.

Figure 20 shows a numerical example of a 3D case and the experimental comparison; the water film has reached the lower edge of the plate and some droplets depart from the film. It can be noticed in this figure that the structures of the water flow at the time of the detachment of the drops are very similar in both cases. So, this type of simulations leads to a better understanding of the processes of formation of droplets under certain flow conditions and their re-entrainment in the main air stream.

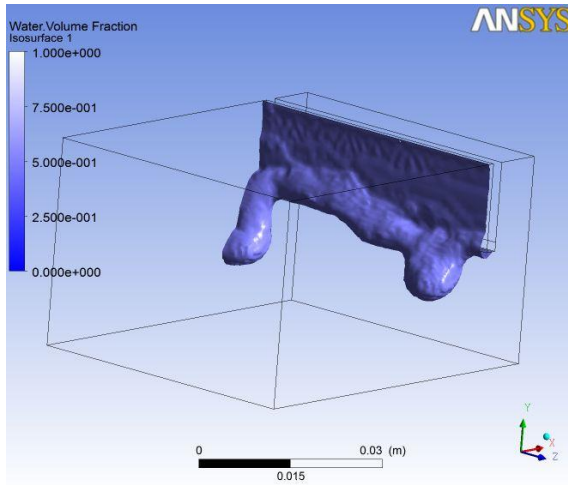


**Figure 20. Detachment of droplets in a 3D numerical case (a) and an experimental case (b).**

## CONCLUSIONS

A numerical study and its experimental validation of the detachment of droplets from an L-shape drift eliminator in a mechanical draft-cooling tower is carried out. This phenomenon is known as breakthrough and it is produced when the air flow profiles, across the entire drift eliminator plane, exceed certain limit velocities and are able to detach some droplets from its walls. To study this problem, different numerical and experimental cases have been analyzed, covering most of the operating conditions of the cooling tower. The presented results for air velocity profiles, water film thickness formed on the plates of the drift eliminator and the droplet size are similar in the numerical and the experimental cases.

Air velocity measurements have determined the velocity profiles in the channel zone, describing a preferential path in the higher velocity zones and some other areas with much lower velocity values.

Results for water film thickness have shown the growth of film thickness as air velocity increases, due to the fact that air holds and accumulates water in the plate leading to higher film thickness.

It has been determined that there are two specific zones in the drift eliminator where, for certain air velocities, the detachment of droplets takes place: the upper edge and the lower edge of the

drift eliminator plates. In both zones, air velocity limits have been found to prevent water droplets going up dragged by the airstream. Moreover, higher film thickness need lower air velocity to form droplets, as seen on air velocity results.

From this study it can be assured that drift eliminators can act as droplet generators, and operating limits for air velocity have been found to avoid this effect.

## ACKNOWLEDGEMENTS

This research is sponsored by the Spanish Government, through the Projects ENE2013-48696-C2-2-R, as well as by the Seneca-Agency for Science and Technology of the Region of Murcia (Spain), through the Project 15184/PI/10.

## REFERENCES

- [1] “A Guide to the Expression of Uncertainty in Measurement” (GUM), ISO/1995
- [2] Anisimov, S., Pandelidis, D. (2014). Numerical study of the Maisotsenko cycle heat and mass exchanger. *International Journal of Heat and Mass Transfer*, 75, 75-96.
- [3] Arienti, M., Wang, L., Corn, M., Li, X., Soteriu, M.C., Shedd, T.A., Herrmann, M. (2010, June). *Modelling wall film formation and breakup using an integrated interface-tracking/discrete-phase approach*. ASME Turbo Expo 2010: Power for Land, Sea, and Air, Glasgow, UK
- [4] Azzopardi, B.J., Sanallah, K.S. (2002). Re-entrainment in wave-plate mist eliminators. *Chemical Engineering Science*, 57,3557-3563
- [5] FLUENT INC. “Fluent 14 Users Guide”.
- [6] FLUENT INC. “Fluent 14 Theory Guide”.
- [7] James, P.W., Wang, Y., Azzopardi, B.J., Hughes J.P. (2003). The role of drainage channels in the performance of wave-plate mist eliminators. *Chemical Engineering Research and Design*, 81, 639-648.
- [8] James, P.W., Azzopardi, B.J., Wang, Y., Hughes, J.P. (2005). A model for liquid film flow and separation in a wave-plate mist eliminator. *Chemical Engineering Research and Design*, 83, 469-477.
- [9] Lan, H., Friedrich, M., Armaly, B.F. (2008). Simulation and measurement of 3D shear-driven thin liquid film in a duct. *International Journal of Heat and Fluid Flow*, 29, 449-459.

- [10] Lucas, M., Ruiz, J., Martinez, M. J., Kaiser, A. S., Viedma, A., Zamora, B. (2013). Experimental study on the performance of a mechanical cooling tower fitted with different types of water distribution systems and drift eliminators, *Applied Thermal Engineering*, 50, 282-292.
- [11] Miller, W. C. (2012). Best practices for minimizing drift loss in a cooling tower. *CTI Journal*, 33, 36-46.
- [12] Zamora, B., Kaiser, A.S. (2012). Simulacion numerica del flujo turbulento de aire con gotas dispersas de agua a traves de separadores de torres de refrigeracion. *Revista Internacional de Metodos Numericos para Calculo y Diseño en Ingenieria*, 28, 148-160.
- [13] Zhou, D. W., Gambaryan-Roisman, T., Stephan, P. (2009). Measurement of water falling film thickness to flat plate using confocal chromatic sensing technique. *Experimental Thermal and Fluid Science*, 33, 273-283.